行政院國家科學委員會專題研究計畫　成果報告

具有低介電常數阻障介電薄膜製程整合之研究(2/2)

計畫類別：個別型計畫
計畫編號：NSC92-2215-E-009-019-
執行期間：92 年 08 月 01 日至 93 年 07 月 31 日
執行單位：國立交通大學電子工程學系

計畫主持人：施敏
共同主持人：張鼎張

報告類型：完整報告
報告附件：出席國際會議研究心得報告及發表論文
處理方式：本計畫可公開查詢

中　華　民　國 93 年 11 月 22 日

行政院國家科學委員會專題研究計畫期末報告

具有低介電常數阻障介電薄膜製程整合之研究(2/2)

Study on the integration of barrier dielectric with low dielectric constant

計畫編號：NSC 92－2215－E－009－041
執行期間：92 年 8 月 1 日至 93 年 7 月 31 日

計畫主持人：施 敏
共同主持人：張鼎張
計畫參與人員：蔡宗鳴、陳紀文、張大山、陳世璋

一.中文摘要

研究積體電路製造技術中的多層導體連線製程。隨著半導體技術的進步，元件的尺寸也不斷地縮小，而多層金屬導體連線的設計，也成為超大型積體電路技術所必須採用的方式。然而，隨著金屬導線層的數目增加及導線間的距離不斷縮小，電子訊號在金屬連線間傳送時，金屬連線的電阻-電容延遲時間(RC delay time)，變成半導體元件速度受限的主要原因。為了降低訊號傳遞的時間延遲，現今已經發展以金屬銅（電阻率為 1.7μΩ-cm）來取代金屬鋁（電阻率為 2.7μΩ-cm）成為導線的連線系統。而在降低電容方面，則朝向低介電常數（ low-k ）材料發展。但是在銅與鑲嵌的製程與電性操作的環境下，溫度與電場的作用，銅極易擴散至低介電常數材料中，並與之發生反應，造成材料特性的劣化與漏電流增大，甚至導致介電質崩潰。因此，在符合製程相容性要求的前提之下，發展具抗銅金屬擴散特性的介電阻障層材料，便成為重要的研究課題。目前一種含氧碳化矽(silicon carbide)材料薄膜，具有低的介電係數(k~3.7)，因此受到廣大的矚目，而被應用於介電阻障層技術中，用來取代傳統具高介電係數的氮化矽(silicon nitride) (k~8)，以降低導線系統的延遲時間。本研究將討論含氧碳化矽膜的基本物性及電性，以及其在製程整合時遇到氧電漿處理以及後段製程受溫度的影響其薄膜對抗銅能力的探討。最後，將樣品放置在低溫的環境下，探討其漏電機制

關鍵詞:低介電數材料, 含氧碳化矽

Abstract

We know that the metal linewidth and spacing decreases with the device scaling, resulting in large RC time delay. Copper is an applicable alternative due to its low resistivity (1.7 μΩ-cm), which is much lower than that of Al (2.7 μΩ-cm). Besides, copper is more resistant to electromigration problem, which is a vital issue in device reliability. The diffusion barrier layer is also served as the etch stop layer during trench formation if necessary. Silicon nitride (SiN) is the currently standard barrier layer material since it has been employed as a masking and passivating layer for a long time against diffusion of metal ions and moisture. Unfortunately, the relative high

dielectric constant (~7) of SiN conflicts with the requirement of low dielectric IMD. Therefore, it is urgently desirable to seek a new barrier layer material. Recently, a newly-developed dielectric barrier material, amorphous SiOC:H has aroused much attention.

In this thesis, we study the fundamental concepts and the intrinsic properties and the effect of O_2 plasma ashing and temperature in BEOL process on the barrier properties of the SiOC:H film against copper penetration. Finally, we let the sample at low temperature and measure its electrical characteristics
Key word: low-k, SiOC:H

二.緣由與目的

Cu has been recognized as the most appropriate alternative for Al as wiring material due to its low electrical resistivity and excellent electromigration resistance [1], [2]. Dual damascene process is the well-accepted patterning technology since it is difficult to pattern Cu film by plasma etching. However, some challenges exist while Cu is to be integrated into the process. It is known that Cu is a serious contamination source for both silicon and silicon dioxide. To prevent Cu from diffusion into IMD, Cu must be sealed by diffusion barriers. The main IMD is essentially some kind of low dielectric constant (low-k) materials. Moreover, a dielectric diffusion barrier layer depositing on Cu wires is necessary to seal Cu and served as the etch stop layer during the via etching of the subsequent layer. This diffusion barrier layer is also served as the etch stop layer during trench formation if necessary. Silicon nitride (SiN) is the currently standard barrier layer material since it has been employed as a masking and passivating layer for a long time against diffusion of metal ions and moisture [3], [4], [5]. Unfortunately, the relative high dielectric constant (~7) of SiN conflicts with the requirement of low dielectric IMD [6]. The impact of SiN on interconnection capacitance becomes more prominent with the decrease of dielectric constant of main IMD. Therefore, it is urgently desirable to seek a new barrier layer material. Recently, a newly-developed dielectric barrier material, amorphous SiOC:H has aroused much attention. It has been widespreadly regarded as the only candidate to replace SiN as the dielectric diffusion barrier and the etch stop layer [7],[8].

In this thesis, we will investigate the intrinsic electric properties of the SiOC:H film and its reliability against Cu contamination.

三.結果與討論

The various concentrations of oxygen were controlled by O_2 gas flow rate during PECVD process. The silicon carbide film was deposited on 8 inch p-type doping silicon wafer with a resistivity of 15-25 Ω-cm. The code name of the pure silicon carbide film in this study is “SiOC”; besides, the code names of silicon carbide films with various flow rate of O_2 gas during PECVD process are “SiOC1”, “SiOC2” and “SiOC3”. The flow rate of O_2 gas for SiOC1, SiOC2 and SiOC3 were 20 %, 30 % and 40 %, respectively. The chamber pressure were 1.5 torr and the chamber temperature were 350°C.

The absorption coefficient obtained from FTIR measurements are shown in Fig. 1, for SiC, SiOC1, SiOC2, SiOC3. The peak at 780 cm^{-1} is identified as Si-C stretching bond. Si-CH_3 bending peak is at 1245 cm^{-1}, Si-H stretching peak is near 2100 cm^{-1}. Note that the peaks at around 1000cm^{-1} may also be attributed to oxygen vibration modes such as Si-O-Si and Si-O-C stretching. [9],[10]. Tab. 1 demonstrates the dielectric constant and refractive coefficient of SiC, SiOC1, SiOC2, SiOC3. The pure silicon carbide film has a dielectric constant about 4.54, and the

dielectric constants of SiOC1, SiOC2, and SiOC3 films were 3.69, 3.55, and 3.49, respectively. Anyhow, we found that the dielectric constants of SiOC1, SiOC2 and SiOC3 are smaller than the pure silicon carbide and will decrease with the increase of the ratio of oxygen/silicon. Fig. 2 shows the XPS curve of SiCO1. Fig. 3 exhibits the AES spectrums of SiCO1.

Metal-insulator-semiconductor (MIS) structures were used to investigate the behavior of basic electrical characteristic. The completed Al and Cu gated MIS capacitors were then bias-temperature-stressed (BTS) at 150°C with gate electrode biases (V_{gate}) . The stress time was 1000 sec, which is long enough for the mobile charges to drift across the stacked insulator layer. The bias was provided by an HP4156 semiconductor parameter analyzer. Notably, the BTS was performed with a continued N_2 purge to prevent the uptake of moisture in the silicon carbide films through testing. In addition, the gate electrode current (I_{gate}) of the MIS structure during BTS measurement was monitored, and the I_{gate}-V_{gate} characteristics were also instantaneously measured from 150 to 25 °C during the lowering course of the temperature after BTS. We will show the current density versus electric field (J-E) and current density versus (I-t) diagrams to demonstrate the effects about BTS (bias-temperature-stress) measuremt. Fig. 4. shows J-E cures of SiC, SiOC1, SiOC2, SiOC3 with Al electrode at RT. The more oxygen concentration in the film, the lower leakage current it is. The more oxygen concentration in the film will cause insulating property increase. Fig. 5 shows J-E cures of SiOC1 with Cu electrode at various temperature. When the temperature increase will cause thermionic emission injection improved. Fig. 6 shows Current v.s. Time curve of SiOC1, SiOC2, SiOC3 with Cu gate during BTS. Oxygen rich SiC film would have better reliability. The lower oxygen concentration has higher leakage current. The leakage current is like electron beam which impact the SiC film. The Si-C bond of SiC film is easier break than Si-O bond. The Si-C break cause the traps to result in Cu diffusion. Therefore, the higher oxygen concentration has lower leakage current.

In this study, sample SiOC1 were experienced O_2 plasma treatment for 3min, 6min and 9min by PECVD (plasma-enhanced Chemical Vapor Deposition) processes in a parallel plate reactor operating at 13.56 MHz. The absorption coefficient obtained from FTIR measurements are shown in Fig 7 for a-SiOC:H films after 3, 6, 9, 12, 15 minutes O_2 plasma treatment. Note that the peak Si-O (1000cm^{-1}) and C-O (2330 cm^{-1}) increased as the treatment time increased. Fig. 8 and Fig. 9 show the AES plot of SiCO1 after 6 and 15 minutes O_2 plasma treatment. When the treatment time increased, we get more oxygen into the film. Fig. 10 illustrated the TDS (thermal desorption spectra) curves of a-SiOC:H films after 3, 6, 9, 12, 15 minutes O_2 plasma treatment, H_2O (m/e=18) could be detected. Fig. 11 shows the C-V curve and Tab. 2 shows the dielectric constant and refractive coefficient for O_2 plasma treatment. The dielectric constant coefficient is increased around 3.9 after O_2 plasma treatment, and V_{fb} is no shift after treatment. Fig. 12 shows J-E curve measured at R.T. of SiCO1 after O_2 plasma treatment with Al electrode. The current density are the same at low electric field (<3 MV/cm), and decreased at high field (>4 MV/cm). Fig. 13 shows J-E curve of SiOC1 after O_2 plasma treatment with Cu electrode. Fig. 14 and Fig. 15 shows BTS of SiOC1 after 9min O_2 plasma treatment with Al and Cu electrode. Fig. 16 demonstrates J-E curve of Al electrode SiOC1 measured at 150°C and R.T. after 3 MV/cm stress with

STD and 3min O_2 plasma treatment. Fig. 17 demonstrates J-E curve of Cu electrode SiOC1 measured at 150°C and R.T. after 3 MV/cm stress with STD and 3min O_2 plasma treatment.

For both Al and Cu electrode samples, we have found that the leakage current is quite comparable before and after BTS. Hence, it is apparent that the electrode material has little impact on the leakage current characteristics. Furthermore, after O_2 plasma treatment, the leakage current is decreased for both Al and Cu electrode. However, from the BTS current-time plot, we observe that the both Al and Cu electrode samples tend to breakdown in high electric field. In addition, the leakage current difference before and after BTS of Cu electrode sample is larger than that of Al electrode. Therefore, we can conclude that the resistance against Cu penetration of SiOC:H film is deteriorated after O_2 plasma treatment even that its leakage current characteristics has been improved.

Furthermore, we are interesting in impacts of thermal annealing of the silicon carbide film, so the oxygen-doped silicon carbide film with Cu or Al metal gate was transferred into furnace at the temperature 400°C for 3 hours in N_2 ambient is showed in Fig. 18 and Fig. 19. After thermal treatment electrical measurement will be also executed. MIS capacitors were used for the determination and evaluation of the permittivity of silicon carbide film. The current-voltage (I-V) characteristics measurements and bias-temperature-stress (BTS) measurement were also executed using MIS structure with HP4156 parameter analyzer. Fig. 20 is J-E cures of SiOC1,SiOC2, SiOC3 with Cu electrode after thermal annealing at RT. Fig. 21 to Fig. 23 is Current v.s Time curve of SiOC1, SiOC2, SiOC3 using Cu gate with intrinsic or after thermal annealing during BTS. The leakage current would decrease after thermal annealing. Heating process will not degrade our silicon carbide films, but seem to eliminate the defects or dangling bonds in the films. Fig. 24 Current v.s. Time curve of SiOC1,SiOC2,SiOC3 with Cu gate after thermal annealing during BTS. Fig. 24 compare with Fig. 6. We will find thermal annealing cause reliability of silicon carbide films improved.

Leakage current behaviors of silicon carbide films can be investigated further on the J-E (leakage current density-electric field) characteristics such as $ln(J) - E^{1/2}$ and $ln(J/E) - E^{1/2}$ plots. The linear variations of the current correspond either to Schottky-Richardson emission or to Poole-Frenkel mechanism. The Schottky-Richardson emission generated by the thermionic effect is caused by the electron transport across the potential energy barrier via field-assisted lowering at a metal-insulator interface. The current density (J) in the Schottky emission can be quantified by the following equation:

$$J = A^* T^2 \exp\left(\frac{\beta_s E^{1/2} - \phi_s}{k_B T}\right) (1)$$

where $\beta_s = (e^3 / 4\pi\varepsilon_0\varepsilon)^{1/2}$, e is the electronic charge, ε_0 is the dielectric constant of free space, ε is the high frequency relative dielectric constant, A^* is the effective Richardson constant, T is the absolute temperature, E is the applied electric field, Φ_s is the contact potential barrier, and k_B is the Boltzmann constant. The schematic of the energy diagram for Schottky emission is displayed in Fig. 25. Besides, the Poole-Frenkel (P-F) emission is due to field-enhanced thermal excitation of trapped electrons in the insulator into the conduction band. The current density is given by:

$$J = \sigma_0 E \exp\left(\frac{\beta_{PF} E^{1/2} - \phi_{PF}}{k_B T}\right) \quad (2)$$

where σ_0 is the conductivity, E is the electric field, $\beta_{PF} = (e^3 / \pi\varepsilon_0\varepsilon)^{1/2}$, and Φ_{PF} is the height of trap potential well. The schematic of the energy diagram for Poole-Frenkel (P-F) emission is illustrated in Fig. 26. The barrier height, however, is the depth of the trap potential well, and the quantity β_{PF} is larger than in the case of Schottky emission by a factor of 2. Distinction between the two mechanisms of leakage current can be done by comparing the theoretical value of β with the experimental one. The β_S and β_{PF} before and after BTS(4MV/cm) for SiOC1, SiOC2 and SiOC3 are listed in Tab. 3. The β_S and β_{PF} before and after BTS(4MV/cm) for SiOC1, SiOC2 and SiOC3 after thermal annealing are listed in Tab. 4. Besides, it can be approximately recognized from the symmetry or asymmetry on J-E curves. Because of the differences of work function and carrier concentration between gate and substrate materials, the J-E curves should be asymmetric in Schottky emission conduction. In other words, Schottky emission conduction is dominated by "electrode". But carries in traps meet the same barrier height no matter in positive or negative bias. That is the reason why Poole-Frenkel emission shows a symmetric J-E curve and its behavior is dominated by "bulk". Based on the above, we also can roughly determine the conduction mechanism by the symmetry about J-E curves.

The extraction procedure of experimental β_s and β_{PF} values are demonstrated on the left half court and right half court. For silicon carbide with Cu or Al gate, the slope ($= \beta / k_B T$) of the straight line portion of curves is showed in Fig. 27. We suppose that there are many defeats and dangling bonds in silicon carbide films essentially and they will clutch and then release the carriers inject from electrode like "traps". If carriers are held by traps, the carriers will form a build-in field against external field due to the Coulomb force. From the following equation:

$$\beta_{\text{ideal}} (E - E_B)^{1/2} = \beta_{fit} E^{1/2} \quad (3)$$

β_{ideal} is the ideal value of β_{PF}, β_{fit} is the experimental β_{PF} exacted by fitting the ln(J/E) versus $E^{1/2}$ plot, E is external field, and E_B is build-in field. Therefore, (E-E_B) which is shown in Fig. 28 is the actual field applied on insulator . If the quantities of traps increase, the E_B will be enhanced and then let the value of β_{fit} decrease. It is universally known that high temperature will let carriers jump out of the potential well easily. In another word, the release efficiency of traps will increase due to higher temperature. From the statistical viewpoint, the probabilities of carriers existing in traps decrease and then make the build-in field E_B faint. We suppose that is the reason why we get a larger value of β_{fit} at high temperature.

Furthermore, ψ_S is the contact potential barrier and ψ_{PF} is the height of trap potential well. For trap states with coulomb potentials, the expression is virtually identical to that of the Schottky emission. The barrier height is the depth of the trap potential well. In addition, we can calculateψ_S the contact potential barrier andψ_{PF} the height of trap potential well at high field. From Eq. (1) and Eq. (2), the current density is given as follow:

$$\ln(J) = \ln A^* + \left(\frac{\beta_s}{k_B}\sqrt{E} - \frac{\Phi_s}{k_B}\right)\frac{1}{T} \quad (4)$$

$$\ln\left(\frac{J}{E}\right) = \ln \sigma_0 + \left(\frac{\beta_{PF} E^{1/2} - \Phi_{PF}}{k_B}\right)\frac{1}{T} \quad (5)$$

We plotted ln(J) v.s. (1/T) and ln(J/E) v.s. (1/T). We can get the slope of the straight line

portion of curve.

$$\Phi_S = \beta_s \sqrt{E} - slope \times k_B \quad (6)$$

$$\Phi_{PF} = \beta_{PF} \sqrt{E} - slope \times k_B \quad (7)$$

The barrier height of SiOC1 was listed in Tab. 5. As shown in Tab. 6 , we found that β_{PF} and ψ_{PF} of SiOC1 will increase after thermal annealing. Fig. 29 is J-E curve of SiOC1 before and after annealing with Cu gate at 150℃. The leakage current decreased after annealing. According to Eq. (3), after thermal annealing, the quantity of traps might decrease and then lower the E_B. We will obtain a large value of β_{fit}. That could be the reason why we got a higher β_{fit} value after thermal annealing. Moreover, the increase of the value of ψ_{PF} might caused by eliminating the shallower traps during thermal annealing and then make the average value of the height of traps potential well rise.

We found that β_{PF} and ψ_{PF} of SiOC1 will increase after thermal annealing is shown in Tab. 7. Fig. 19 is J-E curve of SiOC1 before and after BTS with Cu gate at 150℃. The leakage current decreased after BTS. We will obtain a large value of β_{fit}. According to Eq. (3), after BTS, the quantity of traps might decrease and then lower the E_B.. That could be the reason why we got a higher β_{fit} value after BTS. Furthermore, the increase of the value of ψ_{PF} might caused by eliminating the shallower traps during BTS and then make the average value of the height of traps potential well rise.

we let the sample break down during the bias-temperature-stress (BTS) measurement. Then, we put the sample into low temperature probe station and measure the current-voltage (I-V) characteristics.

Fig. 30 to Fig. 32 show the leakage current density versus electric field (J-E) curve of SiOC1, SiOC2, SiOC3 measured at various temperature of 290°K, 200°K, 100°K with Cu electrode, respectively. From Fig. 30 to Fig. 32, the leakage current is very large both in negative bias and positive bias after BTS. With the decreasing temperature, the leakage current was still very large in negative but was getting smaller in positive bias. The Cu ions existing in silicon carbide would be taken as trap states and could enhance the carriers to transport. The transport of carriers could be divided into three components as follows: thermionic emission, direct tunneling, and trap enhanced thermionic field emission. The third way includes trap enhanced thermionic emission and trap enhanced field emission (indirect F-N tunneling).As shown in Fig. 33 and Fig. 34, the numerous trap states exist in insulator and cause the insulator barrier lowing. The insulator could be regarded as a combination of an ohmic conduction region(caused by numerous trap states exist in insulator) and a very thin insulator. Because of Cu penetration, the interface between ohmic conduction region and thin insulator has a lot of trap states. The electrons can easily transport from trap to trap and weakly depend on temperature. From Fig. 30 to Fig. 32, we can see the more oxygen in the film , the lower leakage current it is in negative bias at the low temperature. It is also show that the more oxygen in the film will has less trap states in the film.

四. 結論

A novel oxygen-doped silicon carbide (SiOC) films has been developed for barrier dielectric applications. The silicon carbide film is hydrophobic due to the existence of $Si\text{-}C_xH_y$ bonds. It provides the silicon carbide a lower dielectric constant than that of typically used $Si_x N_y$ (k~8) as a barrier dielectric and etch stop layer in the interconnection. From the electric analysis, we know that the more oxygen concentration in the film, the lower leakage current it is. It is presents that oxygen concentration in the film

would prevent the Cu ion from diffusing into the film. The leakage current is like electron beam which impact the SiC film. The Si-C bond of SiC film is easier broken than Si-O bond. The Si-C break generate the traps which result in Cu diffusion. Therefore, the higher oxygen concentration has lower leakage current.

After O_2 plasma treatment, the leakage current is decreased for both Al and Cu electrode. However, from the BTS current-time plot, we observe that the both Al and Cu electrode samples tend to breakdown in high electric field. In addition, the leakage current difference before and after BTS of Cu electrode sample is larger than that of Al electrode. Therefore, we can conclude that the resistance against Cu penetration of SiOC:H film is deteriorated after O_2 plasma treatment even that its leakage current characteristics has been improved.

Than we know thermal annealing process would be a critical issue in BEOL fabrication process since the heat provided more possibility of the copper diffusion into low-k IMD & ILD. Therefore, we simulated the BEOL fabrication process by using thermal annealing. From electric analysis, we know the film after thermal annealing is better than intrinsic film. Because of thermal annealing recovered defeat of the film and caused leakage current decreasingly. The leakage current decreased as oxygen concentration increased in the film is still existence.

We suppose that there are many defeats and dangling bonds in silicon carbide films essentially and they will clutch and then release the carriers inject from electrode like "traps". If carriers are held by traps, the carriers will form a build-in field against external field due to the Coulomb force. If the quantities of traps increase, the E_B will be enhanced and then let the value of β_{fit} decrease. It is universally known that high temperature will let carriers jump out of the potential well easily. In another word, the release efficiency of traps will increase due to higher temperature.

After thermal annealing and BTS, the quantity of traps might decrease and then lower the E_B. We will obtain a large value of β_{fit}. That could be the reason why we got a higher β_{fit} value after thermal annealing and BTS. Moreover, the increase of the value of ψ_{PF} might caused by eliminating the shallower traps during thermal annealing and then make the average value of the height of traps potential well rise.

Then we let the sample break down during the bias-temperature-stress (BTS) measurement. Then, we put the sample into low temperature probe station and measure the current-voltage (I-V) characteristics. From the electric analysis, the Cu ions existing in silicon carbide would be taken as trap states and could enhance the carriers to transport. Because of Cu penetration, the interface between ohmic conduction region and thin insulator has a lot of trap states. The electrons can easily transport from trap to trap and weakly depend on temperature. We can see the more oxygen in the film , the lower leakage current it is in negative bias at the low temperature. It is also show that the more oxygen in the film will has less trap states in the film.

五. 參考文獻

[1] N. Awaya, H. Inokawa, E. Yamamoto, Y. Okazaki, M. Miyake, Y. Arita, and T. Kobayashi, "Evaluation of a Cu metallization process and the electrical characteristics of copper-interconnected quarter-micron CMOS," IEEE Trans. Electron Devices, 39, 1206-1212, (1996).

[2] J. Tao, N. W. Cheung, and C. Hu, "Electromigration characteristics of copper interconnects," IEEE Electron Devices

Lett., 14, 249-251, (1993).

[3] T. Lauinger, J. Moscchner, A. G. Aberle, and A. G. Hezel, "UV stability of highest-quality plasma silicon nitride passivation of silicon solar cells, "in Conf. Rec. 25th IEEE Photovoltaic Specialists Conf., 1996, pp. 413-419..

[4] S.M.Hu, "Properties of amorphous silicon nitride, "J. Electrochem. Soc.,vol. 33, pp. 693-698, 1966.

[5] V. Y. Doo, D. R. Nichols, and G. A. Silvery, "Preparation and properties of pyrolytic silicon nitride, "J. Electrochem. Soc., vol. 33, pp.1279-1281, Oct.1966. [6] J. O. Simpson, A. K. St. Clair, Thin Solid Film, 308, p.480 (1997)

[6] "The national technology roadmap for semiconductors, 1999 edition , " Semiconductor International Association, San Jose, CA, 1999.

[7] P. Xu, K. Huang, A. Patel, S. Rathi, B. Tang, J. Ferguson, J Huang, and C. Ngai, "BLOK—A low k dielectric barrier/etch stop film for copper damascene applications," in Proc. IEEE Int. Interconnect Technol. Conf., 1999,pp. 109-111 [9] P. T. Liu, T. C. Chang, Y. L. Yang, Y. F. Cheng, and S. M. Sze, IEEE Trans. Electron Devices, 47, 1733 (2000)

[8] E. Gat, M. A. El Khakani, M. Chaker, A. Jean, S. Boily, H. Pepin, J. C. Kieffer, J. Durand, B. Cross, F. Rousseaux and S. Gugrathi, J. Mater. Res., 7 (1992) 2478.

[9] A. L. S. Loke, C. Ryu, C. P. Yue, J. S. H. Cho, and S. S. Wong, "Kinetics of copper drift in PECVD dielectrics,"IEEE electron device Lett. Vol. 17, p. 549-511, Dec. 1996

[10] *The Application of plasma to chemical Processing*; Baddour, R. F.; Tim mins, R. S., Eds.; Massachusetts Institute of Technology Press: Cambridge, MA, 1967.

	SiC	SiOC1	SiOC2	SiOC3
k	4.54	3.69	3.55	3.49
n	1.88	1.816	1.739	1.661

Tab. 1: Dielectric constant and refractive coefficient of SiC, SiOC1, SiOC2, SiOC3

	STD	3min	6min	9min	12min	15min
k	3.69	3.89	3.74	3.95	4.01	3.87
n	1.816	1.879	1.882	1.966	2.013	2.024
Thickness(A)	984	984	956	943	956	961

Tab. 2: Dielectric constant, refractive coefficient and thickness of SiOC1 after O2 plasma treatment.

	150℃	β_S ($x10^{-23}$)	β_{PF} ($x10^{-23}$)
SiOC1	ideal	3.16	6.32
	Before BTS	4.26	
	After BTS 4MV/cm		5.95
SiOC2	ideal	3.221	6.442
	Before BTS	2.389	
	After BTS 4MV/cm	4.652	
SiOC3	ideal	3.245	6.49
	Before BTS	2.136	
	After BTS 4MV/cm	3.1129	

Tab. 3: β_S and β_{PF} before and after BTS(4MV/cm) for SiOC1

After	150℃	β S (x10^-23)	β PF (x10^-23)
SiOC1	ideal	3.16	6.32
	Before BTS		5.131
	After BTS 3MV/cm		6.221
SiOC2	ideal	3.221	6.442
	Before BTS	3.085	
	After BTS 3MV/cm	3.239	
SiOC3	ideal	3.245	6.49
	Before BTS	2.611	
	After BTS 3MV/cm	3.683	

Tab. 4: β_S andβ_{PF} before and after BTS(4MV/cm) for SiOC1, SiOC2 and SiOC3 after thermal annealing.

Before annealing	ϕ	0.678(ev)
After annealing	ϕ	0.72(ev)
After annealing	After BTS ϕ	0.847(ev)

Tab. 5: **ψ**before and after thermal annealing and after BTS for SiOC1

	Before	After	theoretical
β (10-23)	4.26	5.131	6.32
Φ_{PF}	0.678	0.72	

Tab .6: The changes on β_{PF} and ψ_{PF} after annealing

	Before	After	theoretical
β (10-23)	5.131	6.221	6.32
Φ_{PF}	0.72	0.847	

Table 3-5 The changes on βPF and ψPF after BTS

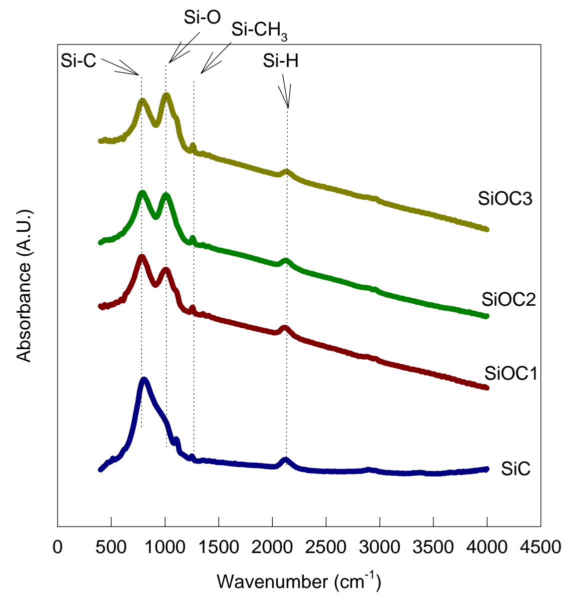

Fig. 1: FTIR absorption spectra for SiC,SiOC1, SiOC2, SiOC3.

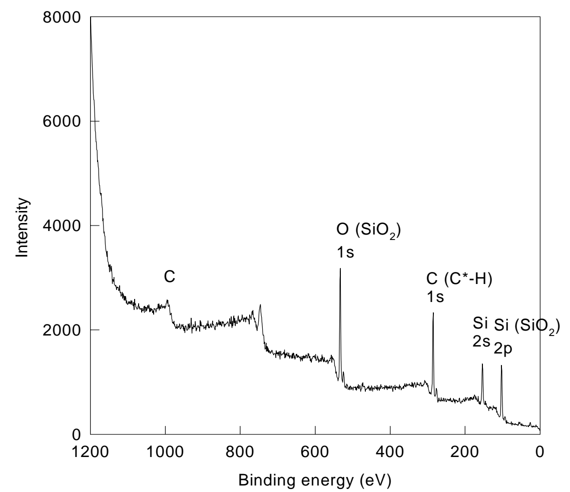

Fig. 2:. XPS curve of intrinsic SiOC1.

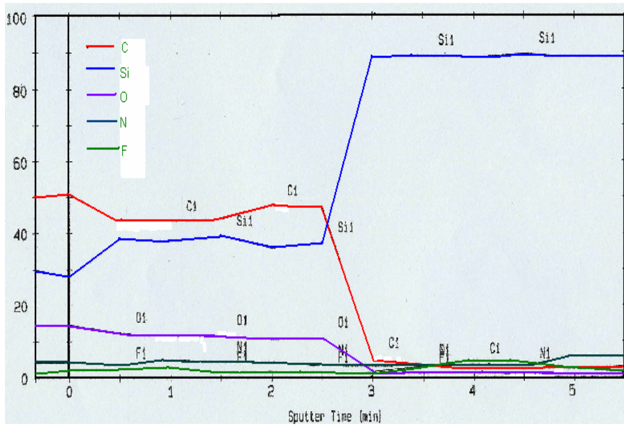

Fig. 3: AES curve of intrinsic SiOC1

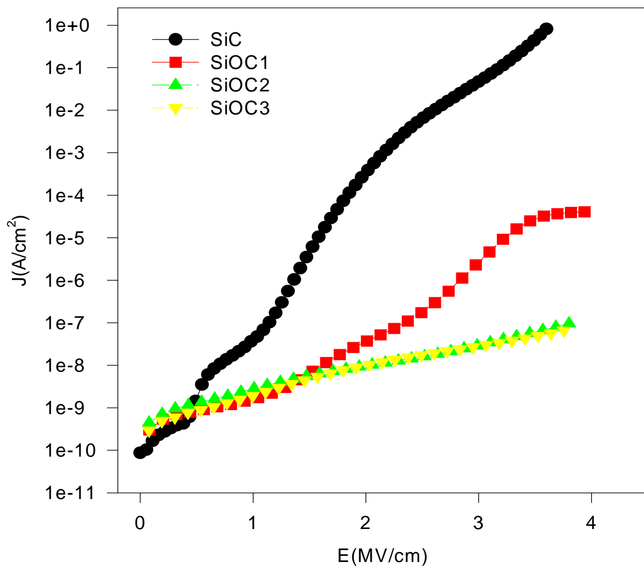

Fig. 4: J-E cures of SiC,SiOC1,SiOC2,SiOC3 with Al electrode at RT

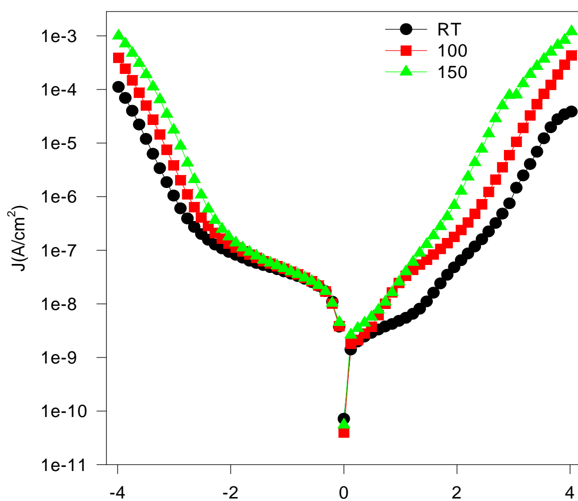

Fig. 5: J-E cures of SiOC1 with Cu electrode

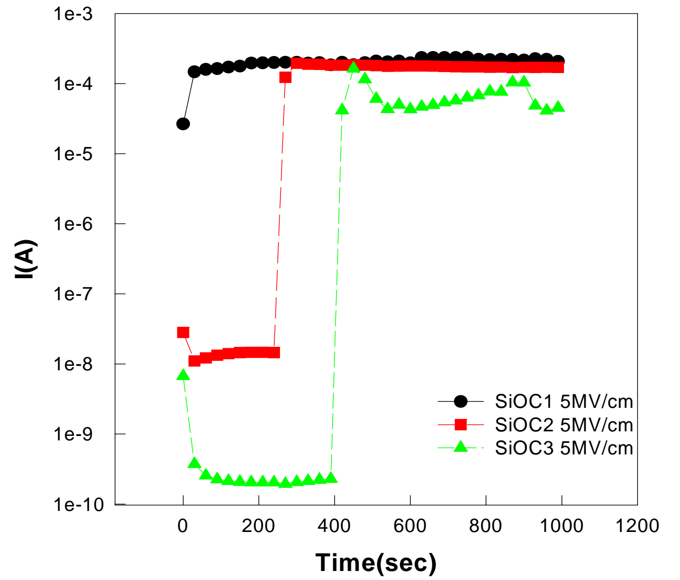

Fig. 6:. Current v.s. Time curve of SiOC1,SiOC2,SiOC3 with Cu gate during BTS

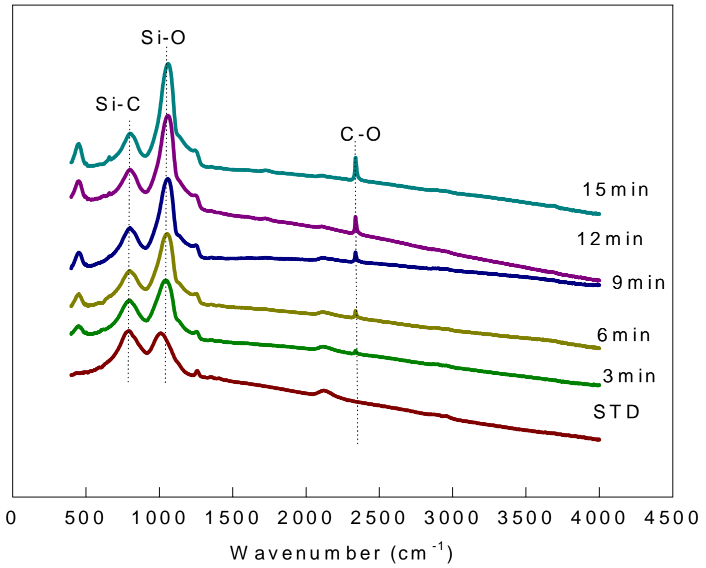

Fig. 7: FTIR of SiOC1 after 3min, 6min, 9min, 12min,15min O_2 plasma treatment.

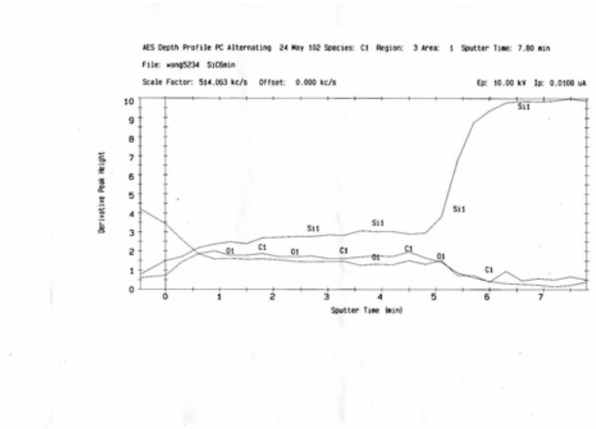

Fig. 8: AES of SiOC1 after 6min O_2 plasma treatment.

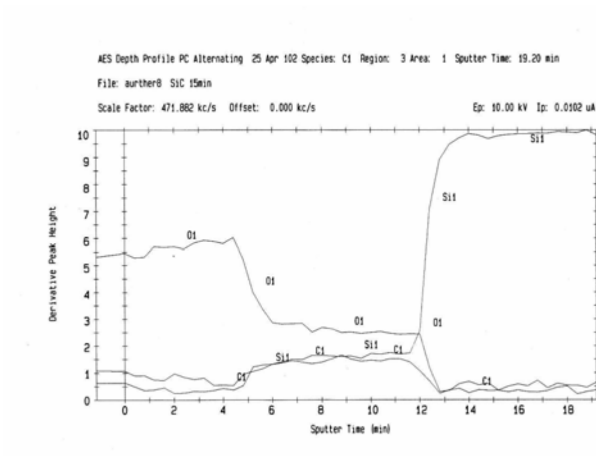

Fig. 9: AES of SiOC1 after 15min O_2 plasma treatment.

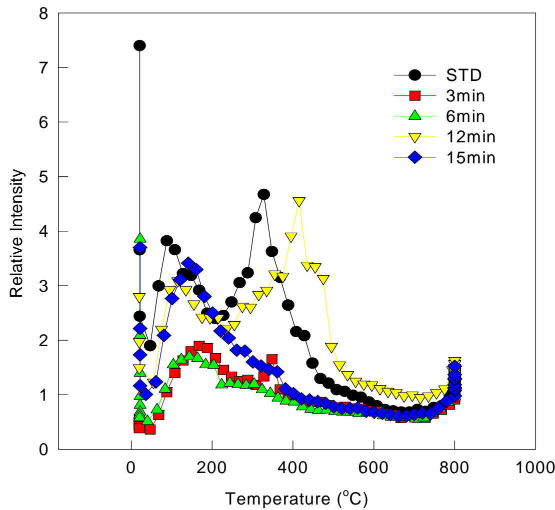

Fig. 10: TDS (m/e=18) of B5-1 after O_2 plasma treatment.

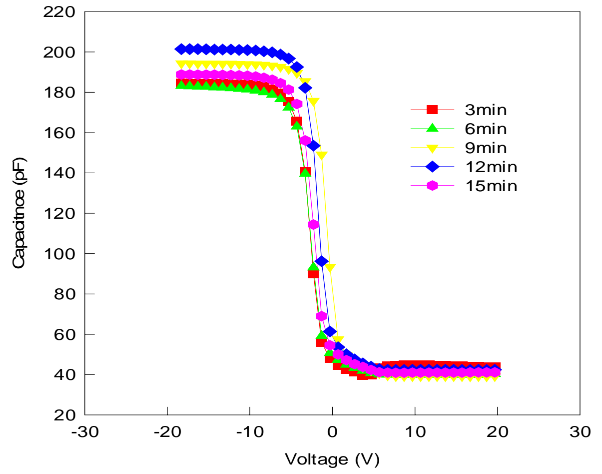

Fig. 11. C-V curve of SiOC1 after O_2 plasma treatment.

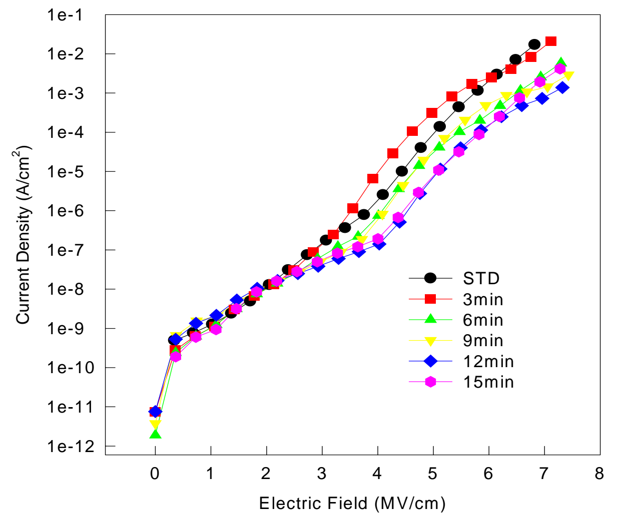

Fig. 12: J-E curve of SiOC1 after O_2 plasma treatment with Al electrode

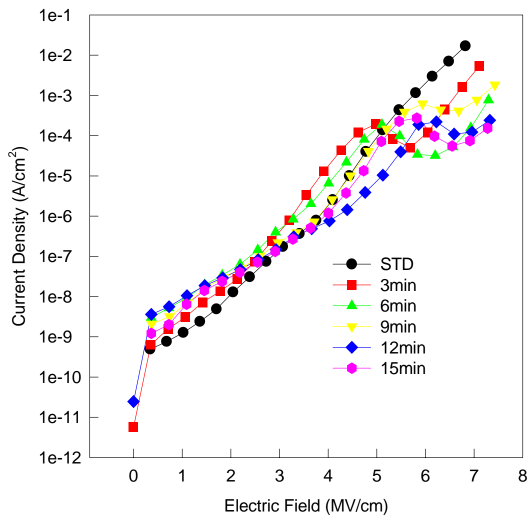

Fig. 13: J-E curve of SiOC1 after O_2 plasma treatment with Cu electrode

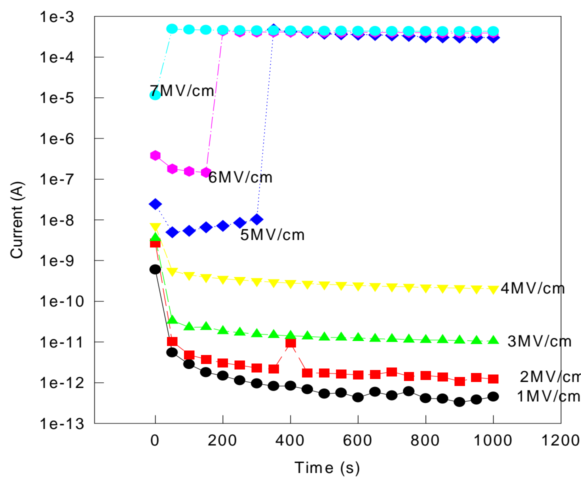

Fig. 14: BTS of SiOC1 after 9min O_2 plasma treatment with Al electrode.

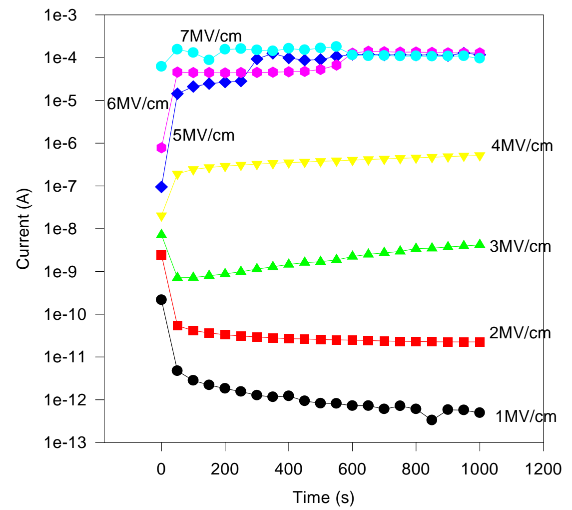

Fig. 15: BTS of SiOC1 after 9min O_2 plasma treatment with Cu electrode

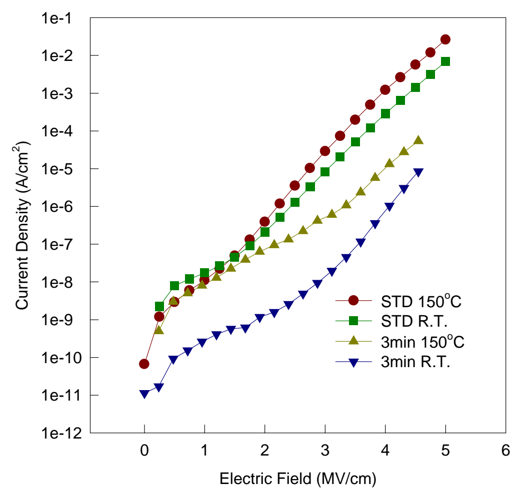

Fig. 16: J-E curve of Al electrode SiOC1 measured at 150°C and R.T. after 3MV/cm stress with STD and 3min O_2 plasma treatment.

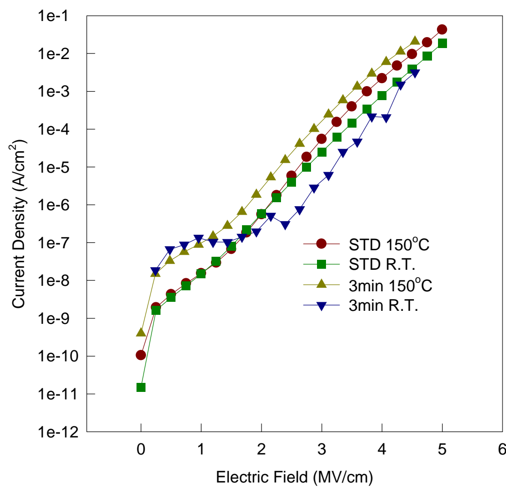

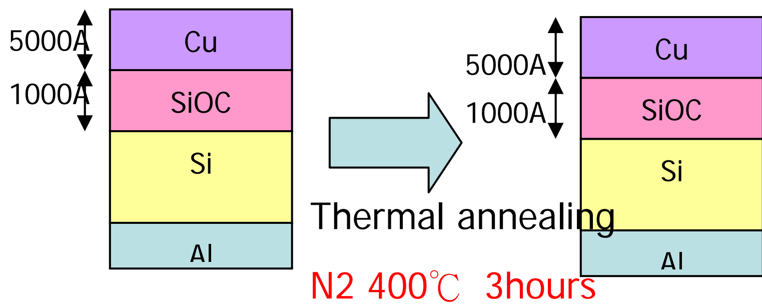

Fig. 19: Show the experiment process

Fig. 17: J-E curve of Cu electrode SiOC1 measured at 150°C and R.T. after 3 MV/cm stress with STD and 3min O_2 plasma treatment.

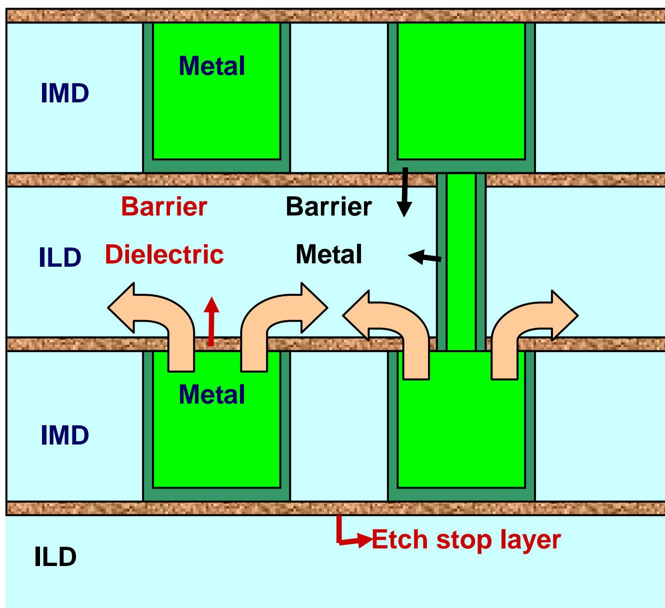

Fig. 18: Schematic of damascene structure with Cu, low-k ILD IMD, barrier dielectric, etch stop layer and barrier metal after thermal annealing

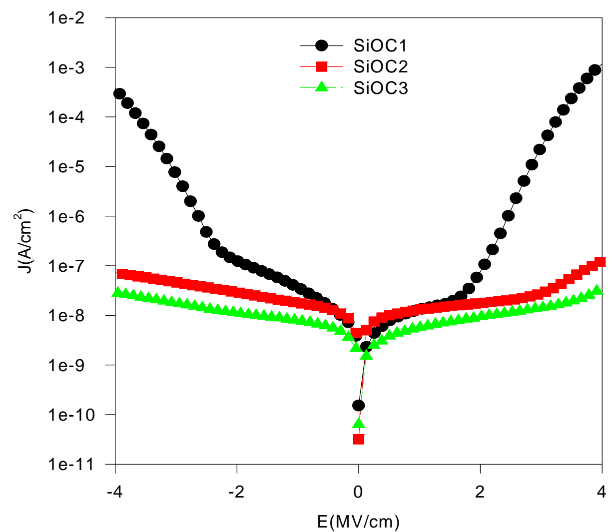

Fig. 20: J-E cures of SiOC1,SiOC2, SiOC3 with Cu electrode after thermal annealing at RT

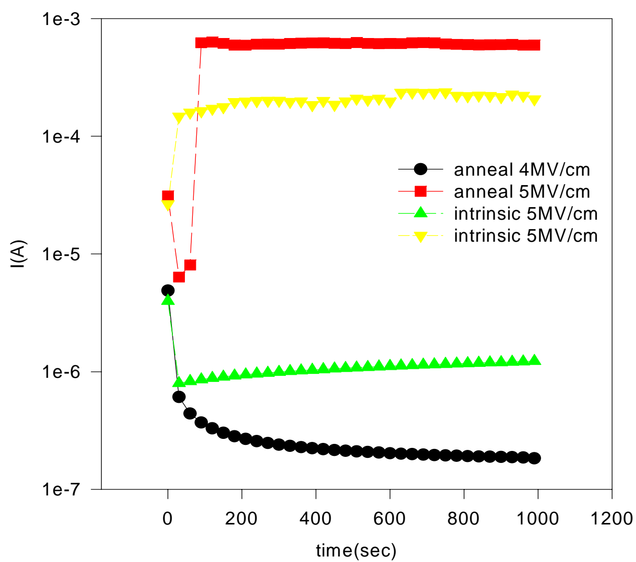

Fig. 21: Current v.s Time curve of SiOC1 using Cu gate with intrinsic or after thermal annealing during BTS

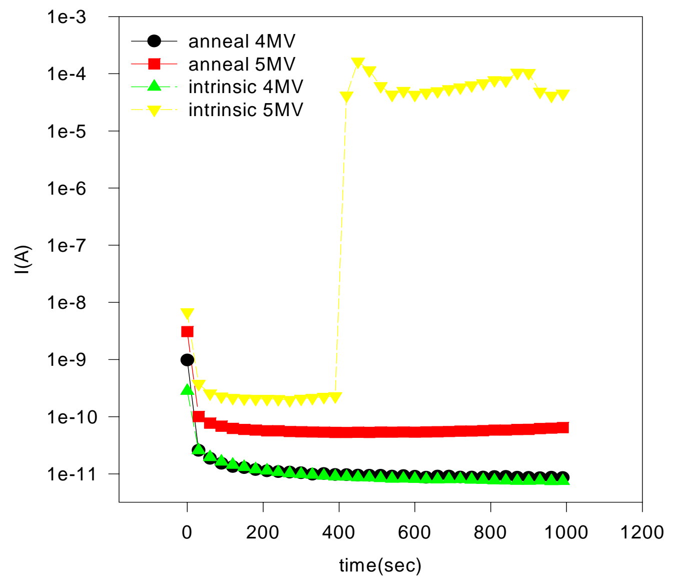

Fig. 23: Current v.s Time curve of SiOC3 using Cu gate with intrinsic or after thermal annealing during BTS

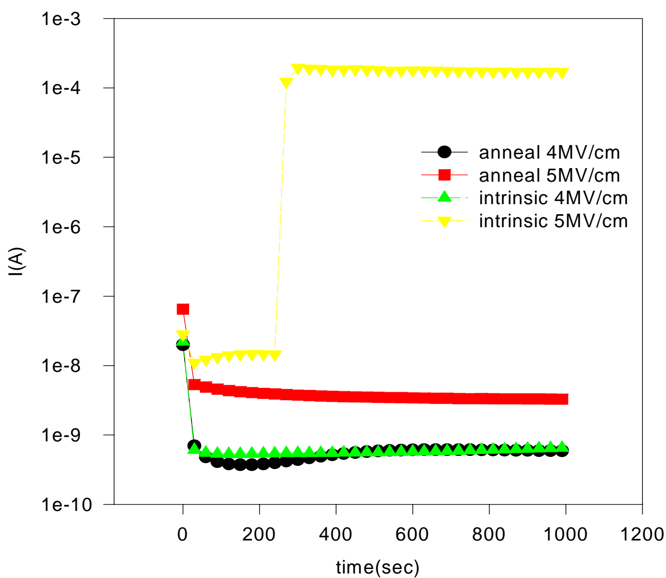

Fig. 22: Current v.s Time curve of SiOC2 using Cu gate with intrinsic or after thermal annealing during BTS

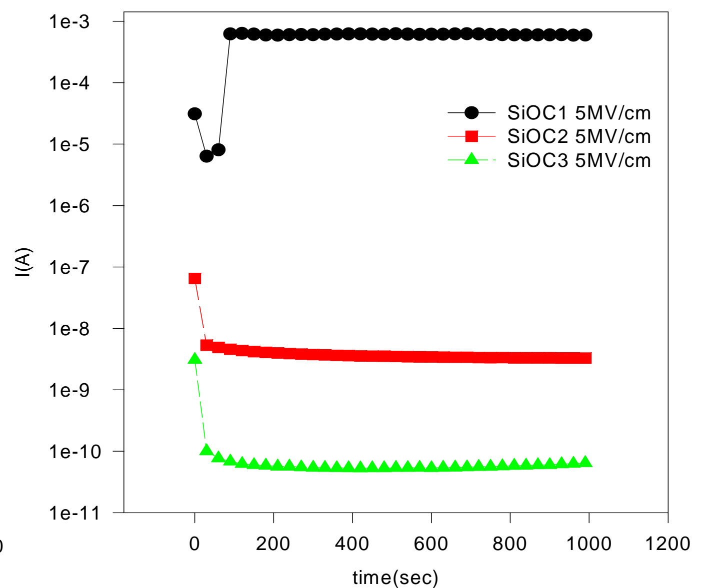

Fig. 24: Current v.s. Time curve of SiOC1,SiOC2,SiOC3 with Cu gate after thermal annealing during BTS

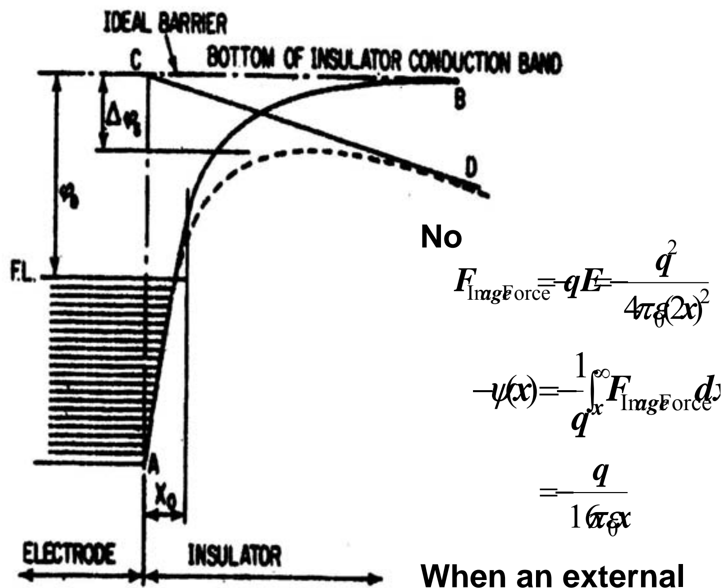

Image-force lowering of a metal-vacuum barrier. This potential energy for an electron is -qψ(x).

No

$$F_{ImageForce} = -qE = -\frac{q^2}{4\pi\varepsilon_0 (2x)^2}$$

$$-\psi(x) = -\frac{1}{q}\int_x^{\infty} F_{ImageForce}\, dx$$

$$= -\frac{q}{16\pi\varepsilon_0 x}$$

When an external

$$-\psi(x) = -\frac{q}{16\pi\varepsilon_0 x} - E_{ext} x$$

$$x_0 = \left(\frac{q}{16\pi\varepsilon_0 E_{ext}}\right)^{1/2}$$

$$\Delta\phi = \left(\frac{qE_{ext}}{4\pi\varepsilon_0}\right)^{1/2}$$

Fig. 25: The schematic of the energy diagram for Schottky emission.

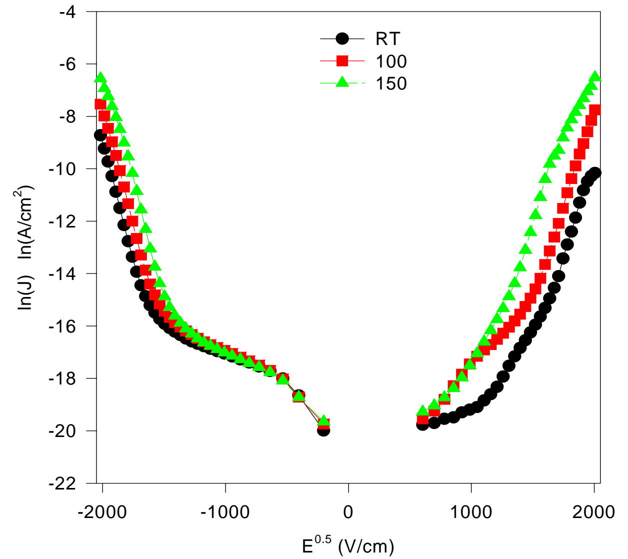

Fig. 27: ln(J)-E0.5 curve of SiOC1 with Cu gate at various temperatures in positive and negative voltage sweep

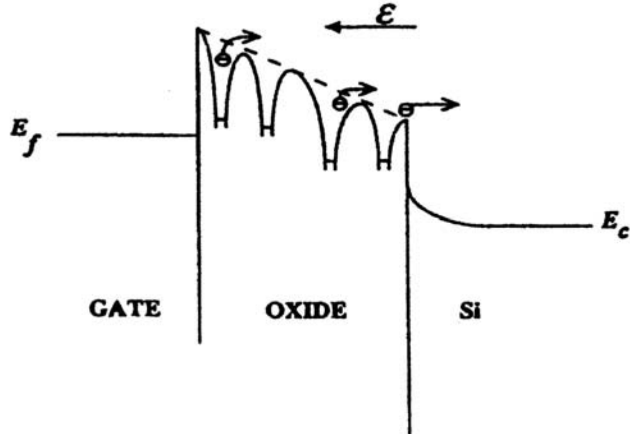

Fig. 26: The schematic of the energy diagram for Poole-Frenkel emission

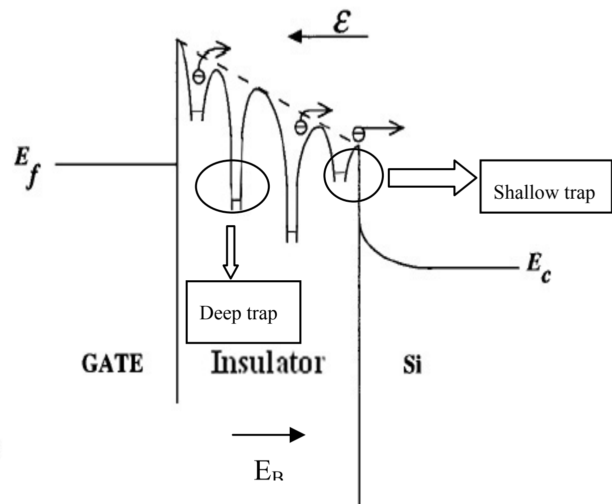

Fig. 28: Band diagram of electron trapping and build-in field

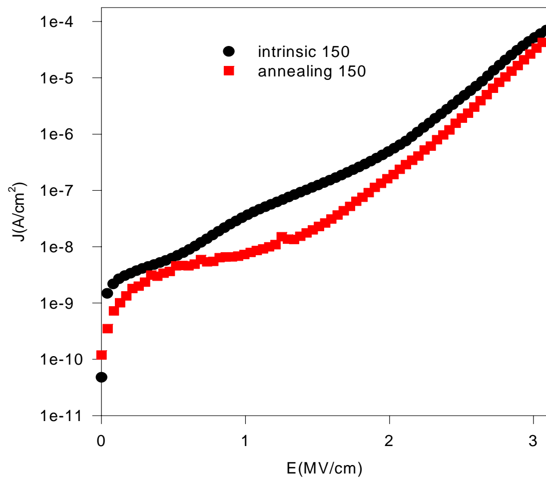

Fig. 29: J-E curve of SiOC1 before and after annealing with Cu gate at 150℃

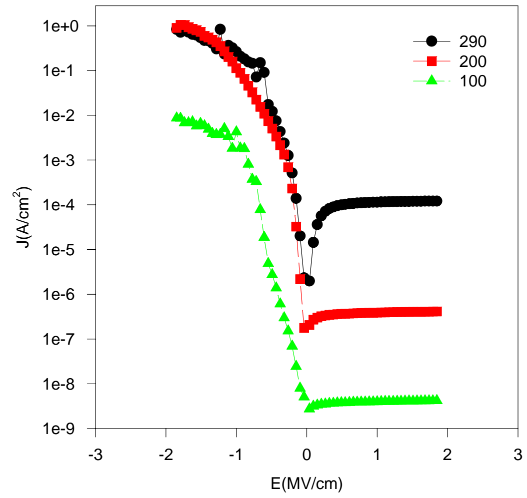

Fig. 31: cures of SiOC2 with Cu electrode at low temperature.

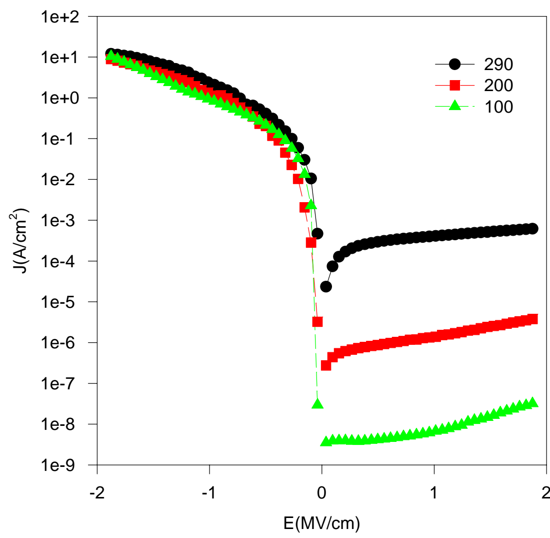

Fig. 30: J-E cures of SiOC1 with Cu electrode at low temperature

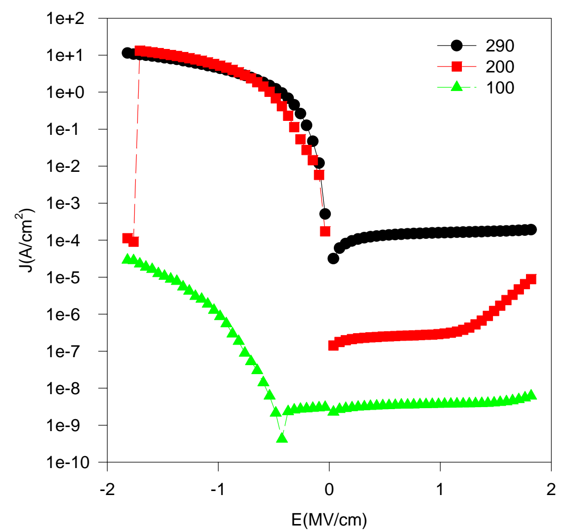

Fig. 32: J-E cures of SiOC3 with Cu electrode at low temperature

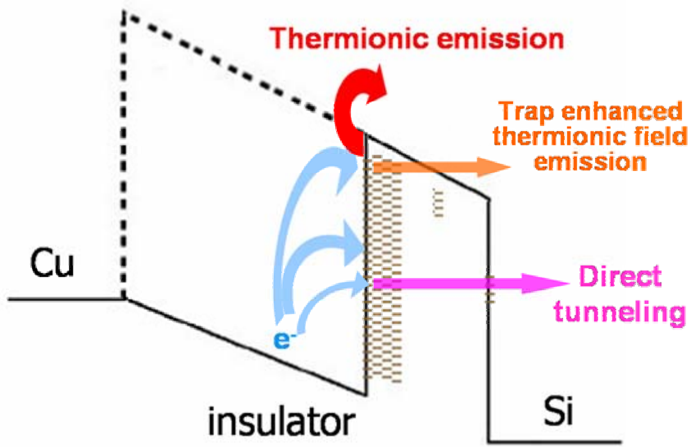

Fig. 33: Band diagrams of the leakage behavior of SiOC (breakdown) in negative voltage sweep.

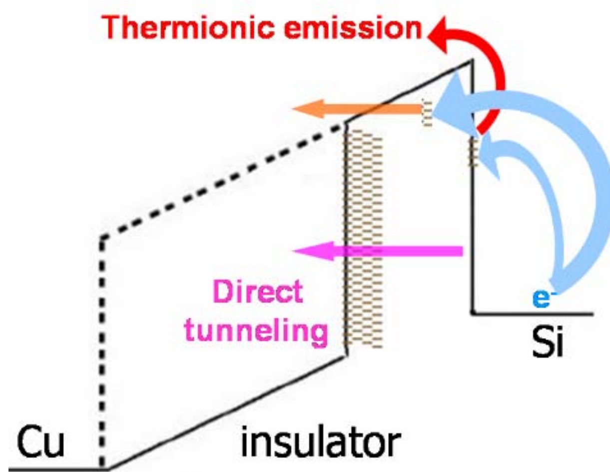

Fig. 34: Band diagrams of the leakage behavior of SiOC (breakdown) in positive voltage sweep

行政院國家科學委員會補助專題研究計畫 ■成果報告
期中進度報告

具有低介電常數阻障介電薄膜製程整合之研究(2/2)

計畫類別：■ 個別型計畫 □ 整合型計畫
計畫編號：NSC 92－2215－E－009－041
執行期間： 92 年 8 月 1 日至 93 年 7 月 31 日

計畫主持人：施 敏
共同主持人：張鼎張
計畫參與人員：蔡宗鳴、陳紀文、張大山、陳世璋

成果報告類型(依經費核定清單規定繳交)：□精簡報告 ■完整報告

本成果報告包括以下應繳交之附件：
□赴國外出差或研習心得報告一份
□赴大陸地區出差或研習心得報告一份
□出席國際學術會議心得報告及發表之論文各一份
□國際合作研究計畫國外研究報告書一份

處理方式：除產學合作研究計畫、提升產業技術及人才培育研究計畫、列管計畫及下列情形者外，得立即公開查詢
□涉及專利或其他智慧財產權，□一年□二年後可公開查詢

執行單位：國立交通大學電子工程研究所

中 華 民 國 93 年 9 月 5 日